Experimental measurements and modelling of vapour-liquid equilibrium of 2,3,3,3-tetrafluoropropene (R-1234yf)- pentafluoropropane (R-245cb) system

Alain Valtz, Jamal El Abbadi, Christophe Coquelet, Céline Houriez

Experimental measurements and modelling of vapour-liquid equilibrium of 2,3,3,3-tetrafluoropropene (R-1234yf) + 1,1,1,2,2-pentafluoropropane (R-245cb) system

Alain Valtz, Jamal El-Abbadi, Christophe Coquelet, Céline Houriez

MINES ParisTech, PSL University, CTP – Centre of Thermodynamics of Processes, 35 rue Saint Honoré, 77305 Fontainebleau Cedex, France

Abstract

Isothermal vapour-liquid equilibrium (VLE) of the R-1234yf + R-245cb binary system were measured using a "static-analytic" apparatus at temperatures from 283.39 to 343.27 K. The data measured were compared with literature data for conformity checking. Albeit both VLE measurement sets are in good accordance, an unexpected behaviour was observed for the relative volatility calculated on the basis of the literature data.

The thermodynamic model used for the calculations reproduces very well R-1234yf + R-245cb VLE data, and is based on a 3-parameter cubic equation of state (denoted by NEoS). This cubic equation of state was associated with the Mathias-Copeman alpha function and van der Waals mixing rules. Comparisons were also done with Peng Robinson EoS with similar alpha function and mixing rules.

Keywords: Equations of state, vapour-liquid equilibrium, refrigerant fluids, fluorinated compounds

Symbols and abbreviations

a	Cohesive energy parameter ($J.m^3.mol^{-2}$)
ARD	Average relative deviation
b	Covolume parameter ($m^3.mol^{-1}$)
EoS	Equation of state
F_{obj}	Objective function
k_{ij}	Binary interaction parameter
m_n	alpha function parameter
NEoS	New equation of state
P	Pressure (MPa) / 1MPa = 10^6 Pa
R	Gas constant ($J.mol^{-1}.K^{-1}$)
T	Temperature (K)
v	Molar volume ($m^3.mol^{-1}$)
x	Liquid mole fraction
y	Vapour mole fraction
Z	Compressibility factor
GWP	Global warming potential
HFCs	Hydrofluorocarbons
HFOs	Hydrofluoroolefins
ODP	Ozone depletion potential

Greek letters

ω	Acentric factor
α	alpha function
Ω_a, Ω_b, Ω_c	Substance depending factors

Subscripts

c	Critical property
cal	Calculated property
exp	Experimental property
i,j	Molecular species
opt	Optimized property
R	Reduced property

1. Introduction

There is now a broad scientific consensus that anthropogenic greenhouse gas emissions are responsible for a developing pattern of climate change, and that the scale of the problem calls for a multifaceted response, including major reductions in global CO_2 emissions. In the energy and industrial sectors, major reductions could be achieved through a combination of demand reduction, fuel substitution, and carbon capture and storage (CCS) [1]. This also includes refrigerant substitution, through using fluids less harmful to the environment.

In the past few years, hydrofluoroolefines (HFOs) have been widely introduced as replacement fluids in many industrial applications due to their low global warming potential (GWP), their zero ozone depletion potential (ODP), and their thermophysical properties. In particular, the 1,1,1,2-tetrafluoroethane (HFC-134a or R-134a), which is widely used in automotive air conditioning, is gradually replaced by the 2,3,3,3-tetrafluoropropene (HFO-1234yf or R-1234yf) due to its low GWP equal to 4 [2] and its thermophysical properties, which are similar to those of R134a. In addition, R-1234yf has low toxicity, low flammability and is chemically stable [3], [4]. The 1,1,1,2,2-pentafluropropane (HFC-245cb or R-245cb) is a by-product resulting in the different synthetic routes of producing R-1234yf [4]–[7]. In addition, normal boiling points of these two refrigerants are quite close [4], [8]–[10], and we need to separate them during the purification process, that implies to know accurately their vapour-liquid equilibrium (VLE) diagram. Although the vapour pressure and PVT data for single compounds R-1234yf and R-245cb have been measured before [4], [8]–[13], VLE data of the mixture R-1234yf + R-245cb are very scarce. And to the best of our knowledge, only one research study [4] has reported the VLE data of this binary system.

In this work, the VLE of the binary system R-1234yf + R-245cb were measured using a "static-analytic" apparatus at temperatures between 283.39 and 343.27 K, in order to fill the gap between existing data, and also to compare with these data.

A 3-parameter cubic equation of state (NEoS) was used to model the VLE results. The NEoS was associated with the Mathias-Copeman alpha function, and van der Waals (vdW) mixing rules, and represents very well the experimental data.

2. Experimental section

2.1. Materials

In Table 1 are listed the refrigerants used for the VLE measurements, with the details about their ASHRAE[1] number, chemical formula, CAS[2] number, along with the name of the supplier and the product purity provided by the supplier. No further purification of the chemical products was needed, only degassing was realised when loading the chemicals into the equilibrium cell.

The critical temperature and pressure, and the acentric factor (ω)[3] of these refrigerants are reported in Table 2.

Table 1. Refrigerants used for the experiments.

Compounds	ASHRAE Number	Formula	CAS Number	Supplier	Purity (vol%)
2,3,3,3-tetrafluoropropene	R-1234yf	$C_3H_2F_4$	754-12-1	Honeywell	> 99.5%
1,1,1,2,2-pentafluropropane	R-245cb	$C_3H_3F_5$	1814-88-6	Synquest	> 99%

Table 2. Critical properties and acentric factors of R-1234yf and R-245cb.

Compounds	T_c/K	P_c/MPa	ω
R-1234yf [a]	367.85 [a]	3.3822 [a]	0.276 [a]
R-245cb [b]	380.38 [b]	3.1483 [b]	0.297 [b]

[a]: Lemmon et al. [14], [b]: Weber and Defibaugh [12]

[1] *ASHRAE: American Society of Heating, Refrigerating and Air-Conditioning Engineers*
[2] *CAS: Chemical Abstracts Service*
[3] *The acentric factor is a conceptual number introduced by Kenneth Pitzer in 1955, and it describes the non-sphericity (centricity) of molecules.*

2.2. Experimental apparatus

2.2.1. Static-analytic apparatus

The equipment used for the VLE measurements is based on a static-analytic method with liquid and vapour phase sampling using capillary samplers ROLSI™. The equipment can be categorized as "Analytical technique with sampling, isothermal AnT" according to Dohrn et al. classification [15]–[17].
The main part of the apparatus is the equilibrium cell, where the two-phase equilibrium takes place. The flow diagram of the apparatus is displayed in Figure 1.

The apparatus is equipped with a thermo-regulated liquid bath in which the equilibrium cell is immersed. The bath ensures the control of the temperature within 0.01 K.
The temperature measurement inside the equilibrium cell is performed using two platinum resistance thermometer probes (Pt100) [18]–[20]: one to measure the temperature at the top of the cell, and the other for the temperature at the bottom of the cell. Two other temperature probes are used to control the temperature inside the thermal presses used to load the chemical products into the equilibrium cell.
The Pt100 probes are connected to a data acquisition unit (HP34970A). The Pt100 probes are calibrated against a 25 Ω reference platinum resistance thermometer (Pt25 - Hart Scientific). The Pt25 reference probe was calibrated by the "Laboratoire National d'Essais de Paris" based on the 1990 International Temperature Scale (ITS 90). The temperature accuracy is estimated to be within ± 0.03 K.
The pressure is measured using one of two pressure transducers (DRUCK, 0–3 MPa, 0–30 MPa) installed on the apparatus. The choice of pressure transducer is dependent upon the maximum pressures generated by the system being characterised. The two pressure transducers are also connected to the data acquisition unit (HP34970A). The pressure transducers were calibrated against a pressure automated calibrator (GE Sensing, model PACE 5000). The pressure accuracy of the transducers is estimated to be within ±0.0004 MPa.

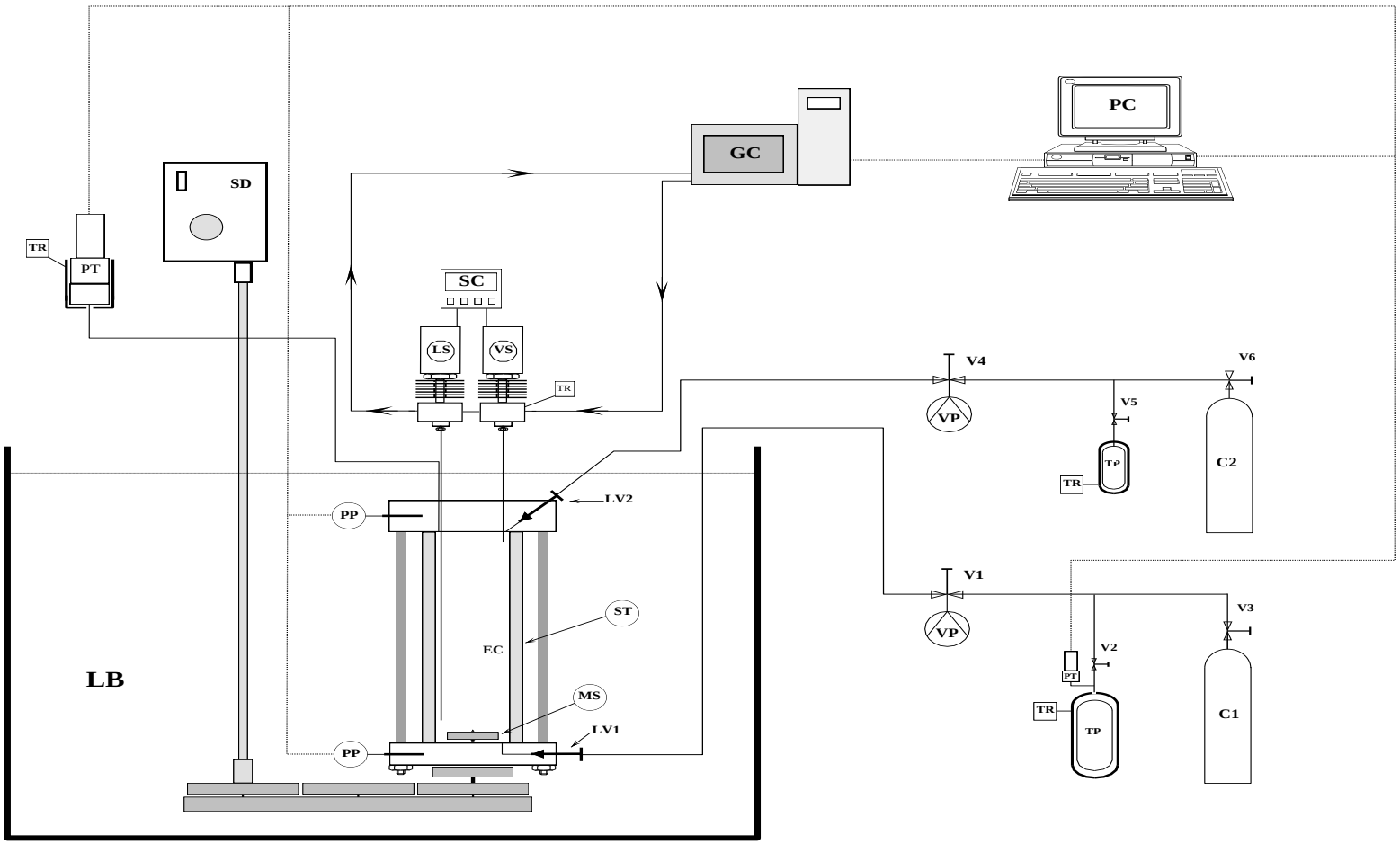

Figure 1. Flow diagram of the "static-analytic" apparatus [18-21].

EC: equilibrium cell; LV: loading valve; MS: magnetic stirrer; PP: platinum resistance thermometer probe; PT: pressure transducer; RT: temperature regulator; LB: liquid bath; TP: thermal press; C1: more volatile compound; C2: less volatile compound; V: valve; GC: gas chromatograph; LS: liquid sampler; VS: vapor sampler; SC: sample controlling; PC: personal computer; VP: vacuum pump.

The compositions of the phases present within the cell are analysed with a gas chromatograph (PERICHROM, model PR2100) equipped with a thermal conductivity detector (TCD). The analytical column within the gas chromatograph is a RESTEK, 1% RT-1000 on Carboblack B, 60/80 mesh (Silcosteel, from Restek; length: 2.4 m; diameter: 2 mm).

The TCD is calibrated by introducing manually known amounts of each pure compound (for the system studied) into the injector of the gas chromatograph, using an automatic syringe (eVOL XR, from SGE). The calibration equation was fitted to relate the response of the TCD to the number of moles of the compound introduced. The mole number accuracy is estimated to be less than 2% for each of the two pure compounds.

2.2.2. Experimental procedure

At ambient temperature, the equilibrium cell and its loading lines are placed under vacuum. A first thermal press is loaded with one of the compounds, and the second thermal press with the other compound. The liquid bath is set to the temperature desired. When the equilibrium temperature is reached (the equilibrium temperature is reached when the Pt100 probes give the same temperature value within their temperature uncertainty for at least 10 minutes), an amount of about 5 cm^3 of the heaviest component (the component with the lower vapour pressure) is introduced into the equilibrium cell. Its vapour pressure is then measured at this temperature [18]–[22].

Then, a given amount of the lightest component (the component with the higher vapour pressure) is introduced step by step in order to increase the pressure inside the cell, leading to successive equilibrium mixtures, in order to have enough points to cover the two-phase envelope.

The equilibrium inside the cell is assumed to be reached when the pressure does not change during a period of 10 minutes within ±0.001 MPa under continuous stirring [18]–[22].

For each equilibrium condition, six or more samples of both vapour and liquid phases are taken using the capillary sampler ROLSI® and analysed in order to verify the repeatability of the measurement. For the complete details about the calibration procedure, the reader can consult the reference [22].

3. Experimental results

3.1. Vapour pressure measurements

The vapour pressures of the pure compounds R-245cb and R-1234yf were measured at temperatures from 278.42 to 356.50 K for R-245cb, and 275.81 to 336.67 K for R-1234yf. The data obtained along with the uncertainties on measurements are listed in Table 3. These latter were calculated following the approach presented in the NIST guidelines [23-25].

Table 2. Experimental vapour pressures of the pure compounds R-245cb and R-1234yf.

R-245cb		R-1234yf	
T/K	**P/MPa**	**T/K**	**P/MPa**
278.42	0.2446	275.81	0.3445
283.05	0.2864	275.82	0.3446
283.25	0.2884	278.21	0.3727
287.61	0.3321	278.21	0.3727
287.65	0.3326	283.03	0.4355
292.85	0.3919	283.04	0.4353
292.86	0.3921	287.94	0.5065
297.57	0.4523	287.94	0.5064
297.60	0.4527	292.76	0.5846
302.75	0.5264	292.82	0.5857
307.05	0.5941	297.70	0.6736
307.11	0.595	297.71	0.6740
312.49	0.6901	302.59	0.7717
312.49	0.6902	302.60	0.7719
317.09	0.7793	307.39	0.8780
317.13	0.7802	307.43	0.8789
322.23	0.8894	312.22	0.9951
322.25	0.8894	312.25	0.9961
327.07	1.0025	317.25	1.1298
327.07	1.0026	322.11	1.2720
331.95	1.1278	322.12	1.2727
331.95	1.1277	327.00	1.4286
336.83	1.2641	327.00	1.4288
336.84	1.2644	331.82	1.5970
341.72	1.4129	331.83	1.5971
341.74	1.4135	336.65	1.7793
346.30	1.5613	336.67	1.7800
346.49	1.5684		
351.62	1.7527		
351.60	1.7522		
356.36	1.9359		
356.45	1.9409		
356.50	1.9427		

$U(T)$[4] = 0.06 K; U(P) = 0.0008 MPa.

[4] *U(X) = u(X, k=2).*

In general, in the DIPPR [26], Equation (1) is used to correlate the pure compound vapour pressure.

$$P = exp\left(E + \frac{A}{T} + Bln(T) + CT^D\right) \quad (1)$$

At the critical point, T = T_C and P = P_C, which gives Equation (2):

$$P_C = exp\left(E + \frac{A}{T_C} + Bln(T_C) + CT_C{}^D\right) \quad (2)$$

Consequently, by considering D = 2, we obtained Equation (3):

$$P = P_C e^{\left(A\frac{1-T_R}{T_R} + Bln(T_R) + C\left(T_R^2 - 1\right)\right)} \quad (3)$$

Here, Pc is the critical pressure of the considered compound, and T_R is the reduced temperature. A, B, and C are three adjustable parameters, whose values are given in Table 4, together with their corresponding deviations. The experimental data were correlated using Equation (3).

Concerning R-245cb, we have included the pure compound vapour pressure data from Shank [13] in the data treatment, in order to cover the maximum range of temperature. According to Table 4, the experimental data are very well correlated by Equation (3) and the corresponding parameters.

Table 4: Equation (3) parameters for the R-1234yf and R-245cb.

Compound	A	u(A)	B	u(B)	C	u(C)	Tmin/K	Tmax/K	ARD%	Bias%
R-1234yf	-19.7088	1.03	-22.3328	1.75	4.9048	0.37	275	337	0.26	0.08
R-245cb	-15.8426	0.74	-15.9154	1.25	3.7025	0.26	232	380	0.28	0.10

3.2. VLE measurements

The binary system R-1234yf + R-245cb was studied at four isotherms ranging between T = 283.39 and 343.27 K. The experimental results for this system, along with the number of samples (n), the standard deviations (σx_1 and σy_1) and the uncertainties on measurements are reported in Table 5.

Table 5. VLE data of the system R-1234yf (1) + R-245cb (2).

P/MPa	n	x_1	σx_1	n	y_1	σy_1
			T = 283.39 K			
0.2891	-	0	-	-	0	-
0.3140	8	0.1550	0.0010	6	0.2110	0.0010
0.3391	6	0.3216	0.0009	7	0.4010	0.0010
0.3723	7	0.5490	0.0010	7	0.6320	0.0030
0.4063	9	0.7670	0.0010	6	0.8190	0.0010
0.4203	11	0.8670	0.0020	9	0.8950	0.0020
0.4402	-	1	-	-	1	-
			T = 303.15 K			
0.5322	-	0	-	-	0	-
0.5747	7	0.1652	0.0007	12	0.2080	0.0010
0.6131	8	0.3187	0.0009	6	0.3858	0.0009
0.6561	5	0.4890	0.0020	6	0.5580	0.0010
0.6969	7	0.6530	0.0010	6	0.7100	0.0030
0.7368	6	0.8110	0.0030	6	0.8460	0.0020
0.7839	-	1	-	-	1	-
			T = 323.30 K			
0.9125	-	0	-	-	0	-
0.9871	6	0.1860	0.0007	7	0.2229	0.0008
1.0535	5	0.3617	0.0006	5	0.4160	0.0030
1.0978	13	0.4760	0.0010	9	0.5340	0.0030
1.1593	4	0.6304	0.0009	5	0.6798	0.0006
1.2192	5	0.7920	0.0020	6	0.8256	0.0006
1.3087	-	1	-	-	1	-
			T = 343.27 K			
1.4615	-	0	-	-	0	-
1.5658	5	0.1830	0.0010	6	0.2160	0.0030
1.6653	3	0.3570	0.0020	5	0.4090	0.0040
1.7393	5	0.4840	0.0020	6	0.5280	0.0040
1.8083	11	0.6050	0.0030	6	0.6540	0.0020
1.9079	7	0.7756	0.0006	7	0.8053	0.0009
2.0577	-	1	-	-	1	-

Expanded uncertainties are: U(T) = 0.06 K; U(P) = 0.0008 MPa; $U(x_1)$ = 0.008; $U(y_1)$ = 0.008.

4. Modelling & discussions

The modelling of vapour pressures and VLE was performed using a newly introduced equation of state (NEoS) [27] associated with the well-known Mathias-Copeman alpha function [28]. The mixing rules used are the classical vdW mixing and combining rules. More details about this model can be found in Appendix or in references [22], [27]. For comparison

purpose, the Peng-Robinson (PR) EoS [29] with the same alpha function and the same mixing rules is also used to model the obtained data.

4.1. Modelling of pure compound properties

For the NEoS, the alpha function parameters m_1, m_2 and m_3, along with the critical compressibility factor Z_c, were fitted on the pure compound data to accurately represent the vapour pressures of these single compounds. The parameters of the NEoS for the R-1234yf come from reference [22]. The average relative deviation (ARD) and the bias are calculated by using Equation (4), relative to data predicted using REFPROP software (labelled asX_{exp} in the equation):

$$ARD(X)\ \% = \frac{100}{N}\left|\sum_{1}^{N}\frac{X_{exp} - X_{cal}}{X_{exp}}\right| \qquad (4)$$

$$Bias\ (X)\ \% = \frac{100}{N}\sum_{1}^{N}\frac{X_{exp} - X_{cal}}{X_{exp}}$$

For the R-1234yf, the ARD is less than 1.4% (bias equal to -1.4%) for vapour pressure and less than 2.2% (bias equal to -0.6%) for liquid densities at saturation. Concerning R-245cb, the parameters were fitted using saturated density data from Shank [13], and their corresponding vapour pressures calculated through the correlation given in Equation (3). The parameters of the NEoS are presented in Table 6. The Figure 2 shows the result of the adjustment for the R-245cb. The ARD is less than 0.3% (bias equal to 0.1%) for vapour pressure, and less than 3.8% (bias equal to 0.6%) for the liquid densities at saturation.

For the PR EoS, the parameters m_1, m_2 and m_3 of the alpha function were determined by using the same protocol and are also presented in Table 6.

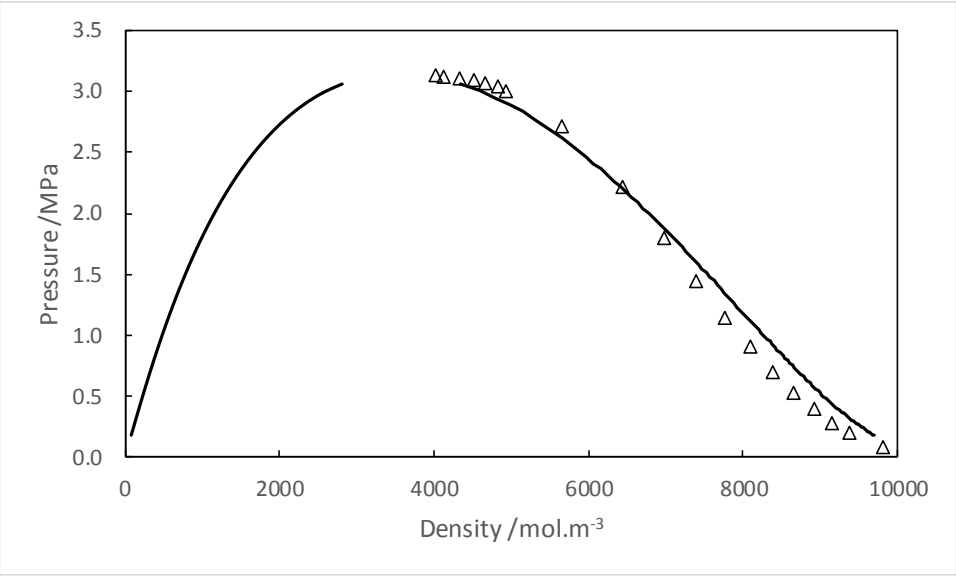

Figure 2: Pressure-density diagram of the R-245cb. Solid line: NEoS prediction with parameters from table 6. (Δ): Data from Shank [13].

Table 6. Pure compound EoS parameters.

Thermodynamic model	Compound	m_1	m_2	m_3	Z_c
NEoS	R-1234yf	0.4636	0.4700	-0.0800	0.28085
	R-245cb	0.5625	-0.4543	3.0585	0.28072
PR EoS	R-1234yf	0.8049	-0.4242	1.7469	-
	R-245cb	0.8920	-1.2280	4.7966	-

Following the modelling of the vapour pressures for the single compounds R-1234yf and R-245cb, a comparison with our measured data and literature data was carried out.

These results are supported by the evaluation of the ARD and bias for the vapour pressures of these two refrigerants (Table 7), for the two models considered in the present paper (NEoS and PR EoS), relative to experimental data. The NEoS reproduces quite accurately both sets of data, as can be seen from Figure 3.

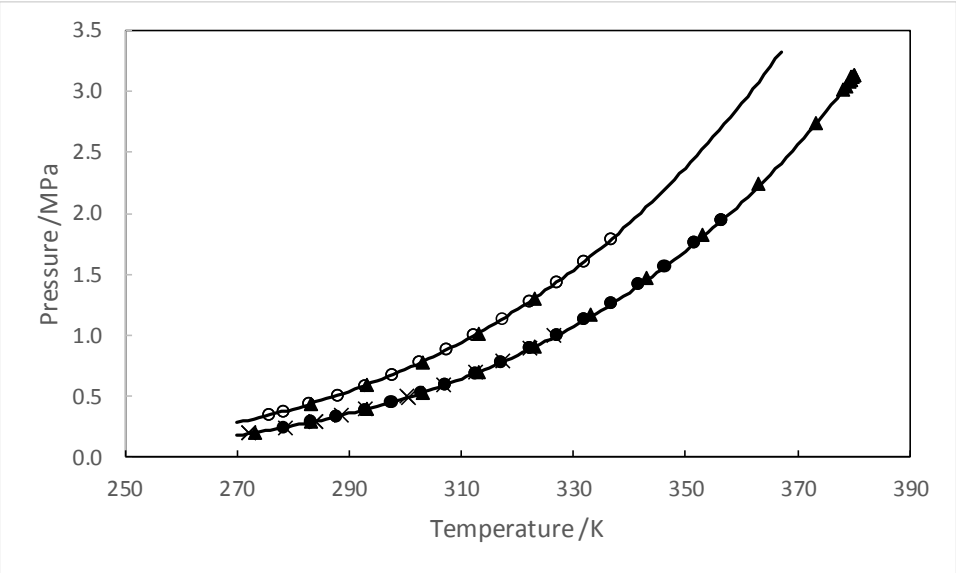

Figure 3. Experimental and calculated vapour pressures of the pure compounds R-1234yf and R-245cb. R-1234yf: (○) This work; (Δ) Hu et al. [30]. R-245cb: (●) This work; (▲) Shank [13]; (×) Weber and Defibaugh [12]. (—) NEoS.

Table 7: ARD and bias for the two EoSs, relative to our measured vapour pressures of R-1234yf and R-245cb.

Compound	Model	ARD (%)	Bias (%)
R-1234yf	NEoS	-0.46	0.46
	PR EoS	0.02	0.01
R-245cb	NEoS	0.26	0.08
	PR EoS	0.12	-0.01

4.2. VLE modelling

The NEoS and PR EoS were used to correlate the experimental data. The binary interaction parameter (BIP) was fitted on experimental VLE data to take into account the effect of intermolecular interactions (Table 8). This system shows a small deviation from Raoult's law and exhibits no azeotropic behaviour in the investigated temperature range, as can be seen on Figure 4.

From comparing the modelling and experiment results (Figure 4 for the VLE and Figure 5 for the relative volatility), it appears that the NEoS reproduces quite accurately the experimental data of both liquid and gas phases for each of the four isotherms studied, with a good representation of the single compound vapour pressures.

From the values of ARD and bias presented in Table 8, we can note that the modelling using the NEoS doesn't improve significantly the results, relative to the PR EoS. However, with the PR EoS, the BIP exhibits a stronger temperature dependency, as compared to NEoS (Figure 6), although the BIP values are small for the two models regardless of the temperature considered (maximum of 0.0081 for the BIP). We have also repeated the data treatment using the NEoS with no temperature dependency of the BIP. Indeed, we previously show in previous paper that an interesting advantage of the NEoS is a non-dependency of the BIP on the temperature, besides a better prediction of densities (Coquelet et al. [27]), see in Appendix. The NeoS has three parameters adjustable on vapour pressure and density data. So, the intermolecular interactions, i.e. repulsive and attractive interactions, are better taken into account. In consequence, for the mixture, it is not necessary to correct strongly with high value of BIP. The value we used for the BIP is k_{12} = -0.00095. The values obtained for ARD on bubble pressure and vapour composition are less than 0.38% (bias 0.3%) and less than 1.15% (bias -0.78%), respectively.

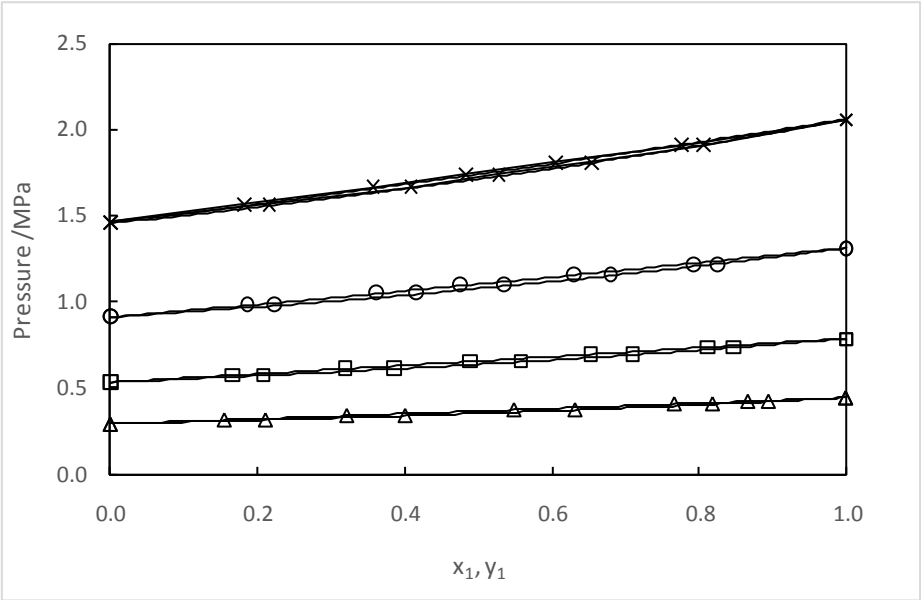

Figure 4: VLE experimental data and modelling for the binary mixture R-1234yf + R-245cb. (Δ) 283.39 K; (□) 303.15 K; (○) 323.30 K; (×) 343.27 K; (—) NEoS.

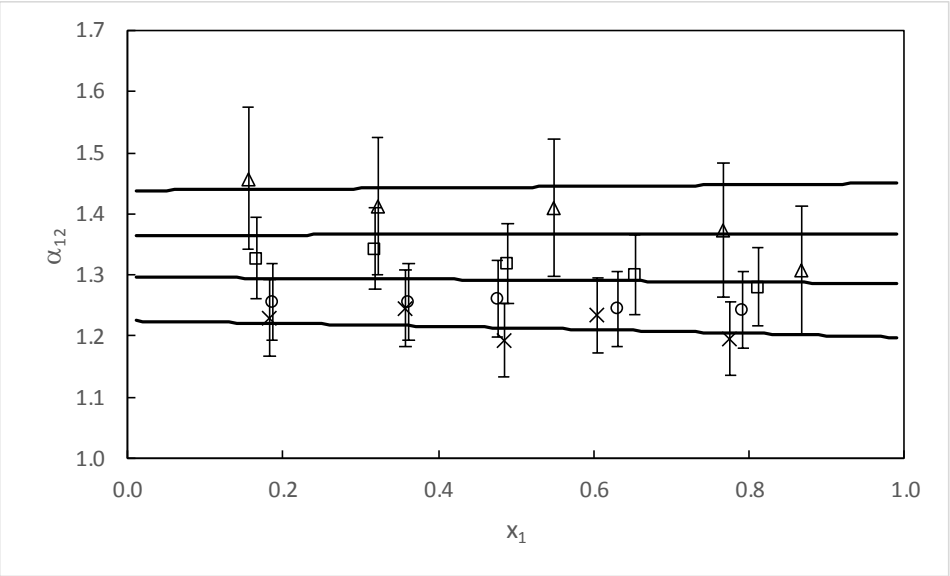

Figure 5: Relative volatility for the binary mixture R-1234yf + R-245cb. (Δ) 283.39 K; (□) 303.15 K; (○) 323.30 K; (×) 343.27 K; (—) NEoS. Error bars: 8%.

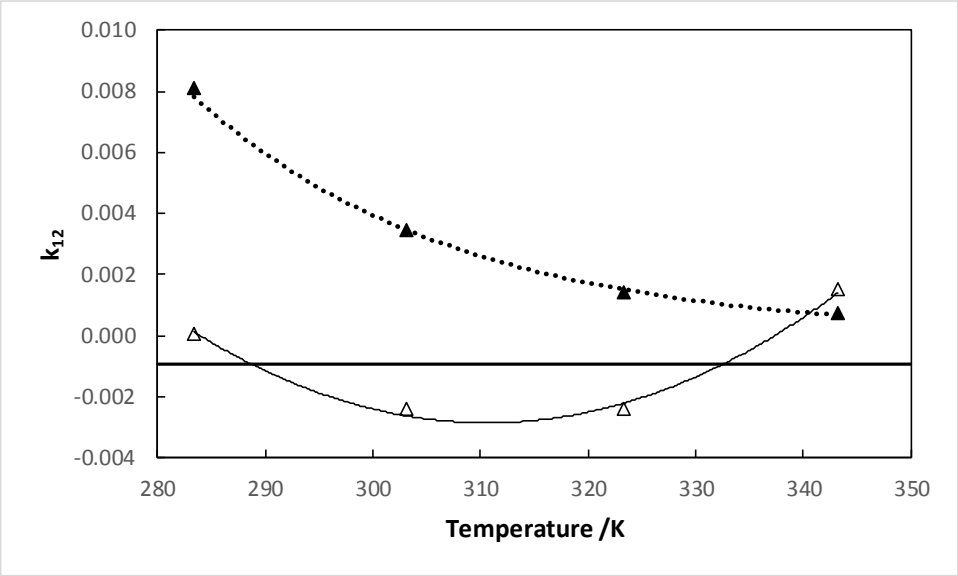

Figure 6: Variation of the Binary Interaction Parameter (BIP) k_{12} as a function of temperature, for the two EoSs. (▲): PR EoS; (Δ): NEoS. Solid line: BIP for NEoS without temperature dependency.

Table 8. ARD and bias for the two EoSs, relative to the measured data of the binary mixture R-1234yf (1) + R-245cb (2).

Model	T/K	k_{12}	ARD P (%)	ARD y1(%)	Bias P (%)	Bias y1(%)
NEoS	283.39	0.00003	0.18	0.91	-0.13	-0.72
	303.15	-0.00241	0.65	1.31	0.65	-1.31
	323.30	-0.00244	0.72	1.30	0.68	-1.30
	343.27	0.00148	0.23	0.57	-0.07	0.22
PR-EoS	283.39	0.0081	-1.00	-1.60	1.00	1.60
	303.15	0.0034	-0.19	-1.85	0.19	1.85
	323.30	0.0014	-0.003	-1.57	0.15	1.57
	343.27	0.0007	-0.06	0.14	0.14	0.58

5. Comparison with literature data

In order to compare our results with literature data, we modelled the data for the system R-1234yf + R-245cb from Yang et al. [4] by using the NEoS, as NEoS and PR-EoS results are quite similar. We used the NEoS with a BIP independent of the temperature.

We calculated the ARD and bias for bubble pressures (0.80% and 0.61%) and vapour mole fraction (1.82% and 1.13%).

On Figure 7, we have plotted the literature data from Yang et al. with our data. Albeit both VLE measurement sets are in good agreement (Figure 7), an unexpected behaviour was observed for the relative volatility calculated from Yang et al. data (figure 8) and the prediction using our NEoS model.

In fact, it is well known that the relative volatility is supposed to vary as a decreasing function (exponential or polynomial) of the liquid molar fraction, that can be verified from the results of our data (as can be seen on Figure 5). On the other hand, the relative volatility calculated from Yang et al. data is varying as an increasing function of the liquid molar fraction, which is somehow unexpected. From analysing further, the data reported by Yang et al. [4], one can notice that for each isotherm, the molar fractions obtained for both vapour and liquid phases are almost the same. And this is somehow strange, given the fact that the measurements are performed through a static-analytic method, and that the odds of obtaining the same composition every time are pretty rare. That leads to think that maybe the experimental

procedure followed is not the one announced by the authors, but rather they proceed by keeping the global composition constant, and they vary the temperature. But, even if this is the case, there should be, in our opinion, a greater difference between the compositions of the points at different temperatures.

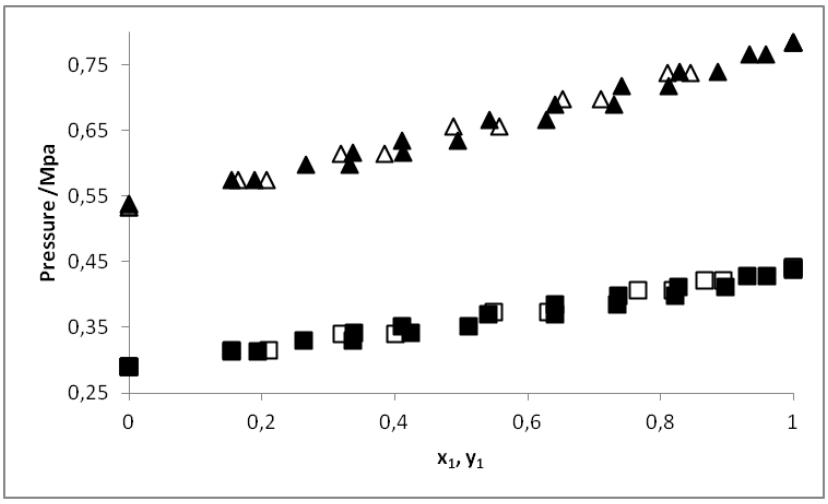

Figure 7: VLE experimental data for the binary system R-1234yf + R-245cb: comparison between this work (empty symbols) and literature data of Yang et al. [4] (filled-in symbols), for isotherms at 283.15 K (squares) and 303.15 K (triangles).

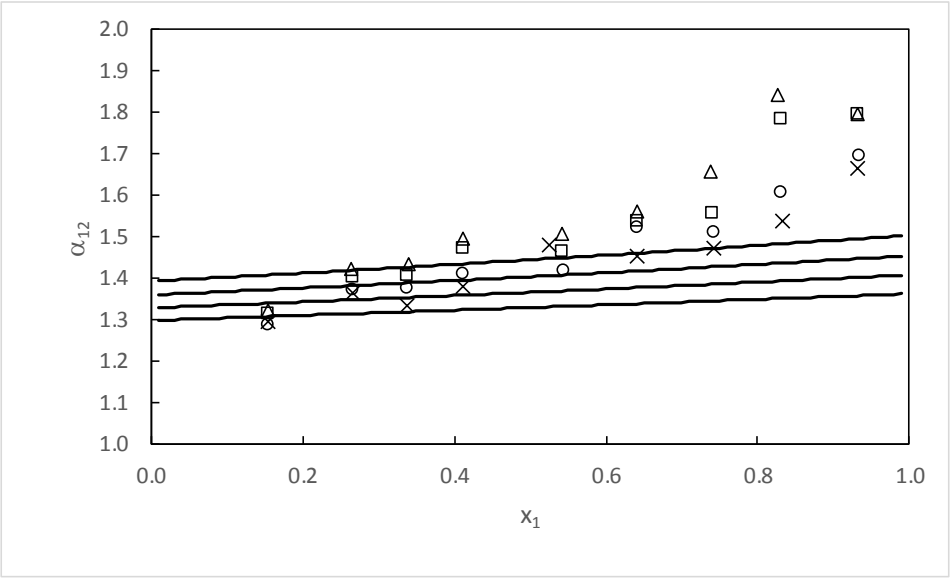

Figure 8: Relative volatility calculated from literature data of Yang et al. [4] for the binary system R-1234yf + R-245cb. (□) 283.15 K; (Δ) 293.15 K; (○) 303.15 K; (×) 313.15 K. (—) NEoS.

6. Conclusions

In this paper, the isothermal VLE of the binary system R-1234yf + R-245cb were measured using a static-analytic apparatus at temperatures from 278.15 to 333.15 K. This system shows a small deviation from Raoult's law and exhibits no azeotropic behaviour in the investigated temperature range.

A 3-parameter cubic equation of state (NEoS) associated with the Mathias-Copeman alpha function, and with vdW classical mixing rules was used for the modelling calculations, and leads to a good description of the experimental results. This work aimed to complete the VLE data for this binary system provided in the literature [4], and in the same time check their consistency. Although these latter two VLE result sets are in good accordance, we found a discrepancy when calculating the relative volatility. Nevertheless, more investigations are needed for VLE data of this system in order to provide data in an extended range of temperatures, and compare the validity of the available data.

Appendix

Description of the NEoS

In order to predict accurately the thermodynamic properties of refrigerants (both pure compounds and mixtures), a new EoS (denoted by NEoS) was developed, based on the modification of the well-known Patel-Teja (PT)EoS [31].

The NEoS is a 3-parameter cubic EoS and is defined by Equation (1).

$$P = \frac{RT}{v - b} - \frac{a(T)}{v^2 + ubv + wb^2} \tag{1}$$

where P is the pressure, T the temperature, v the volume, and R the universal constant for ideal gases. b is the volumetric parameter and a(T) the cohesive energy parameter.

u and w are two parameters defined in order to have: u + w = 0, which was shown to be the optimal combination for liquid density calculations by cubic EoSs [32]. Note that other authors such as Segura et al. [33] work on similar approaches, by the parameterization of u and w, without fixing a relation between them.

Here, u and w are defined as follows (Eq. 2).

$$u = 1 + \frac{c}{b}$$
$$w = -u \tag{2}$$

While the PT EoS [31], [32] [34] and the NEoS have the same definition for u, a different definition for w is chosen in the NEoS in order to fulfil the conditions defined by Ji and Lempe [32], i.e. u + w = 0 (note that in the case of the PT EoS, u + w = 1).

The cohesive energy parameter a(T) depends on the temperature and is defined as follows (Eq. 3):

$$a(T) = a_c \alpha(T) \tag{3}$$

α(T) is the alpha function that will be defined below, and which depends on both the temperature and the substance.

The parameters a_c, b and c of Equations (1) to (3) can conventionally be obtained from the thermodynamic conditions at the critical point, defined as follows (Eq. 4).

$$\left(\frac{\partial P}{\partial v}\right)_{T_c} = \left(\frac{\partial^2 P}{\partial^2 v}\right)_{T_c} = 0 \tag{4}$$

Or from the mathematical constraint (Eq. 5).

$$(v - v_c)^3 = v^3 - 3v_c v^2 + 3{v_c}^2 v - {v_c}^3 = 0 \tag{5}$$

where v_c is the optimized critical volume.

After rewriting Equation (5), we obtain Equation (6).

$$v^3 - \left[\frac{RT}{P} - (u-1)b\right]v^2 + \left[\frac{RT}{P}ub - (w-u)b^2 - \frac{a}{P}\right]v - \frac{RT}{P}wb^2 + wb^3 + \frac{ab}{P} = 0 \tag{6}$$

The parameters a_c, b and c are calculated according to the relations (Eq. 7):

$$a_c = \Omega_a \frac{R^2 {T_c}^2}{P_c}$$

$$b = \Omega_b \frac{RT_c}{P_c} \tag{7}$$

$$c = \Omega_c \frac{RT_c}{P_c}$$

where Ω_a, Ω_b and Ω_c are factors depending on the substance [33]. T_c and P_c are respectively the experimental critical temperature and pressure. We set $T = T_c$ and $P = P_c$ in Equation (6), then the comparison with Equation (5) results in Equation (8).

$$\begin{gathered}\Omega_a = 1 - 3Z_{C,opt}\left(1 - Z_{c,opt}\right) + 3(1 - 2Z_{c,opt})\Omega_b + [2 - (u+w)]{\Omega_b}^2 \\ {\Omega_b}^3 + \left[\left(1 - 3Z_{c,opt}\right) + (u+w)\right]{\Omega_b}^2 + 3Z_{c,opt}^2\Omega_b - Z_{c,opt}^3 = 0 \\ \Omega_c = 1 - 3Z_{c,opt}\end{gathered} \tag{8}$$

$Z_{c,opt}$ is an apparent optimized critical compressibility factor. It is different from the experimental critical compressibility factor Z_c, and adjusted from the experimental VLE data [32], [34], [35] in order to improve the prediction of liquid densities. Here, as u + w = 0, we can simplify Equation (8) to obtain Equation (9).

$$\Omega_a = 1 - 3Z_{C,opt}\left(1 - Z_{c,opt}\right) + 3(1 - 2Z_{c,opt})\Omega_b + 2{\Omega_b}^2$$
$${\Omega_b}^3 + (1 - 3Z_{c,opt}){\Omega_b}^2 + 3Z_{c,opt}^2\Omega_b - Z_{c,opt}^3 = 0 \quad (9)$$

By including the critical compressibility factor in the calculations, better results can be obtained, even though the apparent critical compressibility factor $Z_{c,opt}$ is larger than the experimental one, Z_c.

Mathias-Copeman alpha function

The alpha function used in this work is Mathias-Copeman alpha function [28], defined as follows:

$$\alpha(T) = \left[1 + m_1\left(1 - \sqrt{\frac{T}{T_c}}\right) + m_2\left(1 - \sqrt{\frac{T}{T_c}}\right)^2 + m_3\left(1 - \sqrt{\frac{T}{T_c}}\right)^3\right]^2 ; \quad if\ T < T_c$$
$$\alpha(T) = \left[1 + m_1\left(1 - \sqrt{\frac{T}{T_c}}\right)\right]^2 ; \quad if\ T > T_c \quad (10)$$

where T and T_c are respectively the temperature and the critical temperature. m_1, m_2 and m_3 are three adjustable parameters fitted on the experimental data, and depending on the acentric factor ω. The Mathias-Copeman alpha function is defined by two relations depending if we are above or below the critical temperature, as shown in Eq. 10. In our case, the temperatures of the isotherms are lower than the critical temperature of each pure compound. The analysis of alpha functions is very important and many papers have been published on this topic. We can cite the works from Segura et al. [36] and Pina-Martinez et al. [37]. In these two papers, the authors noticed pitfalls of the Soave-type alpha functions and proposed new mathematical expressions. However, we do not use them in this work and prefer using a common alpha function available in simulation softwares.

The Mathias-Copeman alpha function must satisfy the required conditions of an alpha function, as suggested by several authors [34], [38]:

- It has to be real and positive at all temperatures;
- It has to be a decreasing function, approaching a positive value when the temperature tends to infinity;
- It has to be equal to one at the critical temperature;

- It has to be continuous, as well as its first and second derivatives.

We can verify the conditions of the continuity of the Mathias-Copeman alpha function and its first derivative at the limit of the critical temperature (where the alpha function is defined from two relations). This latter condition is important in order to ensure the continuity of the thermodynamic properties (Coquelet et al. [37]), see Equation (11).

$$\begin{aligned} \alpha_{T<T_c}(T_c) &= \alpha_{T>T_c}(T_c) = 1 \\ \frac{\partial \alpha_{T<T_c}}{\partial T} &= \frac{\partial \alpha_{T>T_c}}{\partial T} = -m_1 \end{aligned} \tag{11}$$

We can notice however that the second derivative of the Mathias-Copeman alpha function presents a discontinuity at the critical point. In fact, a recent paper from Le Guennec et al. [39] defines the different conditions that an alpha function should satisfy (referred to as a consistency test): the alpha function must be positive, decreasing, convex with negative third derivative. According to this study no alpha function from the literature satisfies all the conditions of the consistency test. However, we can notice that in their very recent papers (Le Guennec et al. [40], Pina Martinez et al. [41]), these authors present consistent alpha functions. The Mathias-Copeman alpha function can be associated with any cubic EoS. In this work it was associated with the NEoS.

Density prediction comparison

The figure A presents a comparison between density predicted by REFPROP, PR EoS and the NEOS for the R245cb. The same comparison for R-1234yf is shown on figure B.

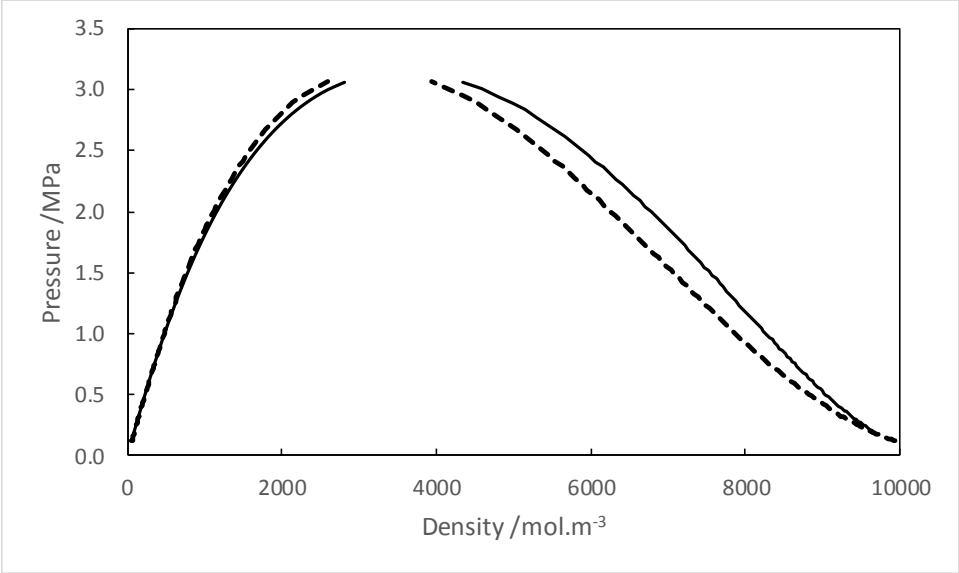

Figure A: Pressure-density diagram of the R-245cb. Solid line: NEoS prediction with parameters from Table 6. Dotted line: PR EoS prediction with parameters from Table 6.

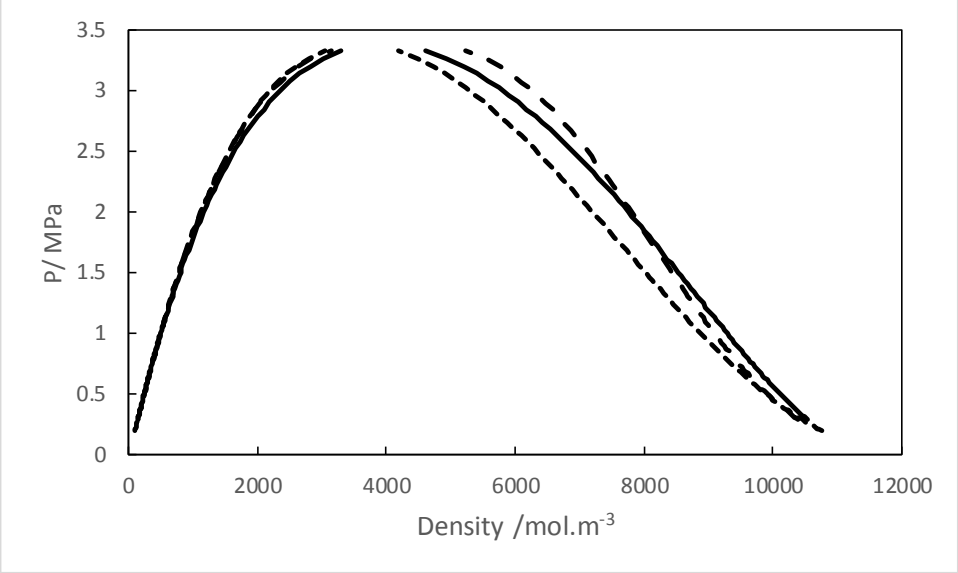

Figure B: Pressure-density diagram of the R-1234yf. Solid line: NEoS prediction with parameters from Table 6. Dotted line: PR EoS prediction with parameters from Table 6. Dashed line: REFPROP 10.0 prediction.

As expected, the NEOS shows better predictive capabilities for densities than PR EoS.

Mixing rules

For the mixtures, the classical vdW mixing and combining rules [29] were used for the calculations. They are defined as follows:

$$a = \sum_{i=1}^{N}\sum_{j=1}^{N} x_i x_j a_{ij}$$

$$a_{ij} = \left(1 - k_{ij}\right)\sqrt{a_i a_j} \quad , \quad i = 1,2 \ldots . N \quad , \quad j = 1,2 \ldots . N \tag{12}$$

$$b = \sum_{i=1}^{N} x_i b_i$$

$$c = \sum_{i=1}^{N} x_i c_i$$

where x_i is the mole fraction of the component i, a_i is the energy parameter, b_i and c_i are the co-volume parameters of the component i, and k_{ij} is the binary interaction parameter. N is the number of components of the system.

The vdW mixing rules were chosen for their simplicity, and ease of computing and also to be able to use a predictive binary interaction parameter k_{ij}.

The binary interaction parameter k_{ij} is fitted on the VLE data of bubble pressure and vapour molar fraction according to the following objective function:

$$F_{obj} = \frac{100}{N}\left[\sum_{1}^{N}\left(\frac{P_{exp} - P_{cal}}{P_{exp}}\right)^2 + \sum_{1}^{N}\left(\frac{y_{exp} - y_{cal}}{y_{exp}}\right)^2\right] \tag{13}$$

where N is the number of data points, P_{exp} the experimental bubble pressure, P_{cal} the calculated bubble pressure, y_{exp} the experimental vapour molar fraction and y_{cal} the calculated vapour molar fraction.

References

[1] Trusler, J. P. M. 2017. Thermophysical Properties and Phase Behavior of Fluids for Application in Carbon Capture and Storage Processes. Annu. Rev. Chem. Biomol. Eng. 8(1), 381–402.

[2] Minor, B., Spatz, M. 2008. International Refrigeration and Air Conditioning Conference at Purdue. Paper No. 2349.

[3] Calm, J.M. 2008. The next generation of refrigerants – Historical review, considerations, and outlook. Int. J. Refrig. 31(7), 1123–1133.

[4] Yang, Z.Q., Kou, L.G., Han, S., Li, C. Hao, Z.J., Mao, W., Zhang, W. Lu, J. 2016. Vapor-liquid equilibria of 2,3,3,3-tetrafluoropropene (HFO-1234yf) + 1,1,1,2,2-pentafluoropropane (HFC-245cb) system. Fluid Phase Equilib. 427, 390–393.

[5] Teinz, K., Manuel, S.R., Chen, B., Pigamo, A., Doucet, N., Kemnitz, E. 2015. Catalytic formation of 2,3,3,3-tetrafluoropropene from 2-chloro-3,3,3-trifluoropropene at fluorinated chromia: A study of reaction pathways. Appl. Catal. B Environ. (165), 200–208.

[6] Wang, H., Bektesevic, S., Merkel, D.C., Tung, H.S., Pokrovski, K.A. 2016. Integrated process to produce 2,3,3,3-tetrafluoropropene. U.S. Patent No. 9,334,206. Washington, DC: U.S. Patent and Trademark Office.

[7] Merkel, D.C., Pokrovski, K.A., Tung, H.S., Wang, H. 2015. Process for producing 2,3,3,3-tetrafluoropropene. U.S. Patent No. 8,975,454. Washington, DC: U.S. Patent and Trademark Office.

[8] Di Nicola, G., Polonara, F., Santori, G. 2010. Saturated Pressure Measurements of 2,3,3,3-Tetrafluoroprop-1-ene (HFO-1234yf). J. Chem. Eng. Data 55(1), 201–204.

[9] Richter, M., McLinden, M.O., Lemmon, E.W. 2011. Thermodynamic Properties of 2,3,3,3-Tetrafluoroprop-1-ene (R1234yf): Vapor Pressure and p – **ρ** – T Measurements and an Equation of State. J. Chem. Eng. Data 56(7), 3254–3264.

[10] Tanaka, K., Higashi, Y., Akasaka, R. 2010. Measurements of the Isobaric Specific Heat Capacity and Density for HFO-1234yf in the Liquid State. J. Chem. Eng. Data 55(2), 901–903.

[11] Fedele, L., Bobbo, S., Groppo, F., Brown, J.S., Zilio, C. 2011. Saturated Pressure Measurements of 2,3,3,3-Tetrafluoroprop-1-ene (R1234yf) for Reduced Temperatures Ranging from 0.67 to 0.93. J. Chem. Eng. Data 56(5), 2608–2612.

[12] Weber, L.A., Defibaugh, D.E. 1996. Vapor Pressure of 1,1,1,2,2-Pentafluoropropane. J. Chem. Eng. Data 41(4), 762-764.

[13] Shank, R. L. 1967. Thermodynamic properties of 1,1,1,2,2-pentafluoropropane (refrigerant 245). J. Chem. Eng. Data 12(4), 474–480.

[14] Lemmon, E. W., Huber, M.L., McLinden, M.O. 2018 REFPROP, Reference Fluid Thermodynamic and Transport Properties, REFPROP, version 10.0. Standard Reference Data Program.

[15] Dohrn, R., Peper, S., Fonseca, J.M.S. 2010. High-pressure fluid-phase equilibria: Experimental methods and systems investigated (2000–2004). Fluid Phase Equilib., 288(1), 1–54.

[16] Fonseca, J. M. S., Dohrn, R., Peper, S. 2011. High-pressure fluid-phase equilibria: Experimental methods and systems investigated (2005–2008). Fluid Phase Equilib. 300(1), 1–69.

[17] Christov, M., Dohrn, R. 2002. High-pressure fluid phase equilibria: Experimental methods and systems investigated (1994–1999). Fluid Phase Equilib. 202(1), 153–218.

[18] Juntarachat, N. Valtz, A., Coquelet, C., Privat, R., Jaubert, J.N. 2014. Experimental measurements and correlation of vapor–liquid equilibrium and critical data for the CO_2 + R1234yf and CO_2 + R1234ze(E) binary mixtures. Int. J. Refrig. 47,141–152.

[19] Williams-Wynn M.D., El Abbadi, J., Valtz, A., Kovacs, E., Houriez, C., Naidoo, P., Coquelet, C. Ramjugernath, D., 2017. Experimental determination of the critical loci for R-23+(n-propane or n-hexane) and R-116+n-propane binary mixtures. J. Chem. Thermodynamics. 108, 84–96.

[20] Valtz, A., Coquelet, C., Baba-Ahmed, A., Richon, D. 2003. Vapor–liquid equilibrium data for the CO_2 + 1,1,1,2,3,3,3,-heptafluoropropane (R227ea) system at temperatures from 276.01 to 367.30 K and pressures up to 7.4 MPa. Fluid Phase Equilibr. 207(1–2), 53–67.

[21] Madani, H. Valtz, A., Zhang, F., El Abbadi, J., Houriez, C., Paricaud, P., Coquelet, C. 2016. Isothermal vapor–liquid equilibrium data for the trifluoromethane (R23) + 2,3,3,3-tetrafluoroprop-1-ene (R1234yf) system at temperatures from 254 to 348 K. Fluid Phase Equilibr. 415,158–165.

[22] El Abbadi, J., 2016. Thermodynamic properties of new refrigerants. PhD thesis, Mines ParisTech, 2016.

[23] Taylor, B.N. 2009. Guidelines for Evaluating and Expressing the Uncertainty of NIST Measurement Results (rev. Ed.). DIANE Publishing.

[24] Zhang, F. 2015. Développement d'un dispositif expérimental original et d'un modèle prédictif pour l'étude thermodynamique des composés soufrés. PhD thesis, MINES ParisTech.

[25] Soo, C.B. 2011. Experimental thermodynamic measurements of biofuel-related associating compounds and modeling using the PC-SAFT equation of state. PhD Thesis, Mines ParisTech.

[26] Daubert, T.E. 1989. Physical and thermodynamic properties of pure chemicals: data compilation. Design Institute for Physacal Property Data (DIPPR).

[27] Coquelet, C., El Abbadi, J. Houriez, C. 2016. Prediction of thermodynamic properties of refrigerant fluids with a new three-parameter cubic equation of state. Int. J. Refrig. 69,418–436.

[28] Mathias, P.M., Copeman, T.W. 1983. Extension of the Peng-Robinson equation of state to complex mixtures: Evaluation of the various forms of the local composition concept. Fluid Phase Equilibr. 13, 91–108.

[29] Peng, D.Y., Robinson, D.B. 1976. A new two-constant equation of state. Ind. Eng. Chem. Fund. 15(1), 59-64.

[30] Hu, P. Chen, L.-X., Chen, Z.-S. 2013. Vapor–liquid equilibria for the 1,1,1,2-tetrafluoroethane (HFC-134a)+1,1,1,2,3,3,3-heptafluoropropane (HFC-227ea) and 1,1,1-trifluoroethane (HFC-143a)+2,3,3,3-tetrafluoroprop-1-ene (HFO-1234yf) systems. Fluid Phase Equilibr. 360, 293–297.

[31] Patel, N.C., Teja, A.S. 1982. A new cubic equation of state for fluids and fluid mixtures. Chem. Eng. Sci. 37(3), 463–473.

[32] Ji, W.R., Lempe, D.A., 1998. A systematic study of cubic three-parameter equations of state for deriving a structurally optimized PVT relation. Fluid Phase Equilibr. 147(1–2), 85–103.

[33] Segura, H., Seiltgens, D., Mejía, A., Llovell, F., Vega, L.F. 2008. An accurate direct technique for parameterizing cubic equations of state. Fluid Phase Equilibr. 265(1–2), 155–172.

[34] Forero G, L.A., Velásquez J, J.A. 2012 The Patel–Teja and the Peng–Robinson EoSs performance when Soave alpha function is replaced by an exponential function. Fluid Phase Equilibr. 332,55–76.

[35] Ji, W.-R. , Stiebing, E., Hradetzky, G., Lempe, D.A. 2007. Extrapolation of VLE data and simultaneous representation of caloric and volumetric properties by means of a cubic 3-parameter equation of state. Fluid Phase Equilibr. 260(1),113–125.

[36] Segura, H., Kraska, T., Mejía, A., Wisniak, J., Polishuk, I. 2003. Unnoticed pitfalls of soave-type alpha functions in cubic equations of state. Ind. Eng. Chem. Res. 42(22), 5662-5673.

[37] Pina-Martinez, A., Privat, R., Jaubert, J. N., Peng, D. Y. 2019. Updated versions of the generalized Soave α-function suitable for the Redlich-Kwong and Peng-Robinson equations of state. Fluid Phase Equilib. 485, 264-269.

[38] Coquelet, C., Chapoy, A., Richon, D. 2004. Development of a New Alpha Function for the Peng–Robinson Equation of State: Comparative Study of Alpha Function Models for Pure Gases (Natural Gas Components) and Water-Gas Systems. Int. J. Thermophys. 25(1), 133-158.

[39] Le Guennec, Y., Lasala, S., Privat, R., Jaubert, J.N. 2016. A consistency test for α-functions of cubic equations of state," Fluid Phase Equilibr., 427, 513–538.

[40] Le Guennec, Y., Privat, R., Lasala, S., Jaubert, J. N. 2017. On the imperative need to use a consistent α-function for the prediction of pure-compound supercritical properties with a cubic equation of state. Fluid Phase Equilib. 445, 45-53.

[41] Pina-Martinez, A., Le Guennec, Y., Privat, R., Jaubert, J. N., Mathias, P. M. 2018. Analysis of the Combinations of Property Data That Are Suitable for a Safe Estimation of Consistent Twu α-Function Parameters: Updated Parameter Values for the Translated-Consistent tc-PR and tc-RK Cubic Equations of State. J. Chem. Eng. Data 63 (10), 3980-3988.